

Causal structure in spin-foams

Eugenio Bianchi^{1,*} and Pierre Martin-Dussaud^{1,2,†}

¹*Institute for Gravitation and the Cosmos, The Pennsylvania State University, University Park, Pennsylvania 16802, USA*

²*Basic Research Community for Physics e.V., Mariannenstraße 89, Leipzig, Germany*

(Dated: September 3, 2021)

The metric field of general relativity is almost fully determined by its causal structure. Yet, in spin-foam models for quantum gravity, the role played by the causal structure is still largely unexplored. The goal of this paper is to clarify how causality is encoded in such models. The quest unveils the physical meaning of the orientation of the two-complex and its role as a dynamical variable. We propose a causal version of the EPRL spin-foam model and discuss the role of the causal structure in the reconstruction of a semiclassical spacetime geometry.

I. MOTIVATION

The information carried by a space-time metric is mainly of causal nature. Indeed, Malament's theorem states that the causal relations between the points of a 4d manifold fully determine the metric, up to a conformal factor given at each point [1]. In quantum models of space-time, the role of the metric is usually played by more fundamental objects, like spins and intertwiners for spin-foams [2, 3]. There, it is less evident to see how causality enters the scene: how is it encoded? The question is of importance to understand more generally whether causality is a fundamental or an emergent property of space-time. Our investigation proceeds as follows:

- II we recall what is meant by causality over a lorentzian manifold and we show how it survives over a simplicial complex;
- III we show how the causal structure can be represented on the dual skeleton;
- IV we show how the causal structure is determined by the dynamics of Regge calculus [4];
- V we elucidate the role of causality at the level of the path-integral over geometries;
- VI we investigate the case of discrete BF theory;
- VII we propose a causal version of the EPRL spin-foam model [5];
- VIII we discuss how the proposed causal EPRL model relates to previous proposals in the literature [6–8].

II. DISCRETE CAUSAL STRUCTURE

The geometry of a lorentzian manifold is fully encoded in the metric g . The signature of g is either $(-, +, +, +)$

or $(+, -, -, -)$. It is generally hold that this freedom is a pure convention, with no physical consequences. However, for the rest of our work, it is useful to let this choice open and write the signature as $(\eta, -\eta, -\eta, -\eta)$ with $\eta \in \{-1, +1\}$.

The *causal structure* of g can be decomposed into two sub-notions that we call *bare-causality*¹ and *time-orientability* (see [9] for a standard reference).

Bare-causality.

We call *bare-causality* the property of each tangent space at any point of the manifold, to be partitioned into three classes of tangent vectors: time-like, space-like and null. Formally, the classes are equivalence classes for the relation:

$$u \sim v \iff \text{sign } g(u, u) = \text{sign } g(v, v), \quad (1)$$

where u and v are tangent vectors. Specifically, we call *time-like* the class of vectors for which

$$\text{sign } g(u, u) = \eta \quad (2)$$

and *space-like* the one for which

$$\text{sign } g(u, u) = -\eta. \quad (3)$$

The definition of bare-causality is local, in the sense that it makes sense at each point of the manifold, but it can also be formulated as a global property. The 'bare-causal structure' of a lorentzian space-time consists in the possibility to say, given any two points, whether they are space-like, time-like or null separated. To be clear with the definitions, two points are time-like separated if they can be joined by a smooth curve whose tangent vectors are time-like all along. It is important that the curve is smooth, because otherwise one could turnaround sharply and draw a time-like curve between any two points.

*Electronic address: ebianchi@psu.edu

†Electronic address: [martindussaud\[at\]gmail\[dot\]com](mailto:martindussaud[at]gmail[dot]com)

¹ The denomination is ours. Surprisingly enough, the literature does not seem to have already named this specific property. It usually calls it simply 'causality', but we need another word to be accurate.

Time-orientability.

On top of bare-causality, one can define a notion of *time-orientability*. At a local level, time-orientability is the property of time-like vectors to be divided into two classes: past and future. Formally, the two classes are equivalence classes of time-like vectors for the relation:

$$u \sim v \iff \text{sign } g(u, v) = \text{sign } g(v, v). \quad (4)$$

In the case of bare-causality, the information contained in the metric g alone enables to distinguish one from another the three classes of time, null and space, without ambiguity. This is not the case for time-orientability: the two classes defined by (4) are perfectly symmetric. Thus, the denomination ‘past’ or ‘future’ is arbitrary as long as no external arrow of time is imposed additionally. So we can pick a reference vector u_0 (the arrow of time), label the two classes by $\omega \in \{-1, +1\}$ and say that the time-like vector v is in the class ω if

$$\text{sign } g(u_0, v) = \omega \eta. \quad (5)$$

To fix the language, we declare that $\omega = +1$ is the future, so that u_0 is future-pointing.

As done previously, the local definition of time-orientation can be turned into a global one by requiring continuity across the classes at different points. Then, space-time is said to be time-orientable if it is possible to continuously define a division of time-like vectors in past and future classes. It is then possible to say that a point lies in the future of some other. As a consequence, one can define the *causal future* $I^+(p)$ and the *causal past* $I^-(p)$ of a point p . Again, the arrow of time, i.e. the labelling of ‘past’ or ‘future’, is conventional, e.g. attached to a specific choice of reference vector u_0 , but it is not a geometric property of the metric.

Time-orientability is conceptually different from bare-causality. However, any lorentzian metric locally defines light-cones with both a bare-causal and a time-orientable structure. So the conceptual difference is often overlooked and the term of ‘causality’ is used indifferently to talk about either notions or both. Yet, it is important to have the distinction clear in mind, especially when moving to quantum models, because we expect the lorentzian metric to make way to new objects, while the underlying physical notions may survive.

Discrete bare-causality.

At a discrete level, consider a lorentzian 4-simplicial complex Δ , i.e. a set of minkowskian 4-simplices nicely glued together [4]². It is again possible to define the notions of bare-causality and time-orientability, both at a local and at a global level.

Each 4-simplex σ comes with an embedding in Minkowski space-time. It is bounded by 5 tetrahedra, each of them having a unique normal 4-vector N , of unit norm and directed outward. A priori, N can be time-like, space-like or null. Two nearby 4-simplices share exactly one common tetrahedron T . The two 4-simplices are said to be time-like separated if N (computed with respect to any of the two 4-simplices) is time-like. A similar definition holds for space-like and null separation.

Unfortunately, this local notion of bare-causality fails to extend straightforwardly to distant 4-simplices. Indeed, one could be tempted to say that two distant 4-simplices are time-like separated if there exists a sequence of time-like separated nearby tetrahedra in-between. However, this definition fails, because, for instance, two space-like separated nearby tetrahedra could be connected by a common time-like separated nearby tetrahedron. In the previous continuous case, the smoothness of the time-like curve was preventing such a pathology, but this is not anymore possible in the discrete case. The difficulty can be circumvented by first introducing a local notion of time-orientability.

Discrete time-orientability.

A tetrahedron is said to be space-like if it is embedded within a space-like hyperplane. In this case, its 4-normal N is time-like. Time-orientability is the property that the space-like boundary tetrahedra of a 4-simplex can be divided into two classes, by the following relation

$$T_1 \sim T_2 \iff \text{sign}(N_1 \cdot N_2) = \text{sign}(N_1 \cdot N_1), \quad (6)$$

where the dot denotes the minkowskian scalar product. A choice of time-orientation consists in saying which class is called past or future (relatively to the 4-simplex).

At a global level, we say that Δ is time-orientable if there exists a consistent choice of time-orientation for each 4-simplex, so that each space-like tetrahedron has an opposite time-orientation relatively to each of the two 4-simplices that bounds it: if a tetrahedron is in the future of a 4-simplex, it should be in the past of another.

Given two 4-simplices, σ_1 and σ_2 , sharing a space-like tetrahedron T , we say that σ_2 is in the future of σ_1 if T is in the future of σ_1 (hence in the past of σ_2). This definition allows us to define straightforwardly a notion of causal future and causal past of a 4-simplex: σ_2 is in the future of σ_1 if there exists a future-oriented chain of 4-simplices in-between. This definition encompasses the notion of time-like separation for distant 4-simplices that was initially looked for. Thus, both bare-causality and time-orientability are defined locally and globally in the discrete setting.

III. CAUSALITY ON THE DUAL SKELETON

The previously defined discrete causal structure can be easily represented on Δ_1^* , the dual 1-skeleton of Δ . Δ_1^* is built from Δ by replacing each 4-simplex by a vertex,

² We leave the rigorous definition of ‘nicely glued together’ unspecified here as it does not affect directly our investigation. See [10] for details.

each tetrahedron by an edge and forgetting about triangles, segments and points of Δ .

Bare-causality discriminates between space-like and time-like edges³, while time-orientability provides an orientation to the time-like edges. Overall, causality is then represented by

1. An arrow from past to future on time-like edges.
2. No arrow on space-like edges.

In the following, we assume that all tetrahedra are space-like, which implies that all N are time-like. Dually, it means that all the edges of Δ_1^* carry an arrow. This simplifying assumption is made in many of the formulations of spin-foams. It is important to note that this condition automatically implements some implicit assumptions about the fundamental causal structure of space-time. Indeed, this assumption erases any local notion of bare-causality: all nearby 4-simplices are time-like separated. Thus, at the most local level, the primacy is granted to time-orientability. The notion of bare-causality only emerges at a more global level as follows: given two distant vertices, if one is not in the past of the other, then they are said to be space-like separated.

Dual causal set.

In mathematical terms, Δ_1^* is a 5-valent *simple oriented graph*⁴. Its *transitive closure* defines a *poset* (partially ordered set). The elements of the poset are the vertices of Δ_1^* and the partial order \leq comes from a unique extension of the set of arrows with the following properties:

1. Reflexivity: $v \leq v$ (by convention).
2. Anti-symmetry: $v_1 \leq v_2$ and $v_2 \leq v_1$ imply $v_1 = v_2$.
3. Transitivity: $v_1 \leq v_2$ and $v_2 \leq v_3$ imply $v_1 \leq v_3$.

In most reasonable cases, the poset of Δ_1^* is *locally finite*, meaning that for any pair of vertices (v_1, v_2) , the so-called *causal diamond* $\{v \mid v_1 \leq v \leq v_2\}$ is a finite set. Such a poset is a *causal set*, as defined originally in [11].

We have shown, without much surprise, that the discretisation of a lorentzian manifold naturally carries a causal set structure. Causal set theory takes the causal set structure as a starting point. Then, the question naturally poses itself as to whether or not it is possible to reconstruct Δ_1^* from its associated causal set only. Given a causal set, one can derive a notion of neighbourhood by declaring that two vertices x and y , such that $x \leq y$,

are next to each other if there is no $z \neq x, y$ such that $x \leq z \leq y$. In other words, the neighbourhood relations are obtained by a *transitive reduction* of the causal set, i.e. a graph with the fewest possible arrows and the same ‘reachability relations’ as the causal set. Interestingly, for a finite directed acyclic graph⁵, such a transitive reduction is unique. However, *the transitive reduction of the transitive closure is not the identity*. Thus, it is not possible to recover Δ_1^* from the causal set by transitive reduction. In other words, the notions of neighbourhood for causal set theory and for discrete lorentzian geometry, as described over Δ_1^* , are not the same.

Similarly, the conformal factor, which is an important piece of information of the metric, can arise in several different ways. In causal set theory, it emerges by counting the number of vertices within a given causal diamond [11, 12]. In discrete lorentzian geometry, it can be given by the lorentzian volume of the 4-simplices, which requires additional input, not deducible from the causal set alone. For instance, the additional information can be provided by coloring each vertex with a real number (the 4-simplex volume), or by coloring each edge with the volume of the corresponding tetrahedron, or by introducing faces and coloring them with the area of the corresponding triangles. The latter option is of course relevant for spin-foam models as discussed also in [6, 13–16].

To work algebraically with the causal structure, it will soon appear convenient to express the orientation of the edges as follows. Given a vertex v , we define the orientation of an edge⁶ $e \in v$ with respect to v as

$$\varepsilon_v(e) \stackrel{\text{def}}{=} \begin{cases} -1 & \text{if } e \text{ is incoming} \\ 1 & \text{if } e \text{ is outgoing.} \end{cases} \quad (7)$$

This convention is similar to the earlier choice in equation (5) to call $\omega = 1$ the future. We define a *causal structure on the 1-skeleton* as an assignment of an orientation $\varepsilon_v(e)$ to each pair (v, e) such that $e \in v$, under the constraint

$$\varepsilon_{v_1}(e) = -\varepsilon_{v_2}(e), \quad (8)$$

where v_1 and v_2 are the two end-points of e . The latter condition expresses the fact that an incoming edge, with respect to one vertex, is outgoing with respect to the other.

Causal wedges.

We have seen that the causality of Δ can be read on the edges of Δ_1^* . Now we are going to show that it can also be read equivalently on the wedges of the dual 2-skeleton Δ_2^* .

³ We deliberately ignore the null case, which does not seem to shed much light on our investigation.

⁴ A *directed graph* is given by a set of vertices and a set of ordered pairs of vertices (arrows). It is said *simple* if there are no arrows from a vertex to itself. It is said *oriented* if there is at most one arrow between any two vertices.

⁵ A directed acyclic graph is a directed graph with no directed cycles, which means, in causal language, no closed time-like curves.

⁶ We denote indifferently $e \in v$ or $v \in e$ when the vertex v is an endpoint of the edge e .

To proceed, let's go back to the 4-simplicial complex Δ . A pair $w = (t, \sigma)$ such that $t \in \sigma$ is called a *wedge*. Given a wedge w , there exists exactly two tetrahedra $T_1, T_2 \in \sigma$ that share t , to which are associated the normals N_1 and N_2 . The *dihedral angle* of w is defined as

$$\theta_w \stackrel{\text{def}}{=} \text{sign}(N_1 \cdot N_2) \cosh^{-1}(|N_1 \cdot N_2|). \quad (9)$$

This definition is a natural extension of the notion of dihedral angle from euclidean to minkowskian geometry. Its absolute value $|\theta_w|$ depends only on the absolute value of the scalar product $|N_1 \cdot N_2|$ of the normals. On the other hand, its sign depends on if the relative time-orientation of the two normals

$$\text{sign}(\theta_w) = \begin{cases} +\eta & \text{if } N_1 \text{ and } N_2 \text{ are co-chronal} \\ -\eta & \text{if } N_1 \text{ and } N_2 \text{ are anti-chronal.} \end{cases} \quad (10)$$

When the normals are co-chronal (resp. anti-chronal), the wedge is said to be *thick* (resp. *thin*). At the level of the wedges, causality shows up as follows: a thick wedge encloses a time-like region, while a thin wedge encloses a space-like region (see fig. 1). The thin/thick distinc-

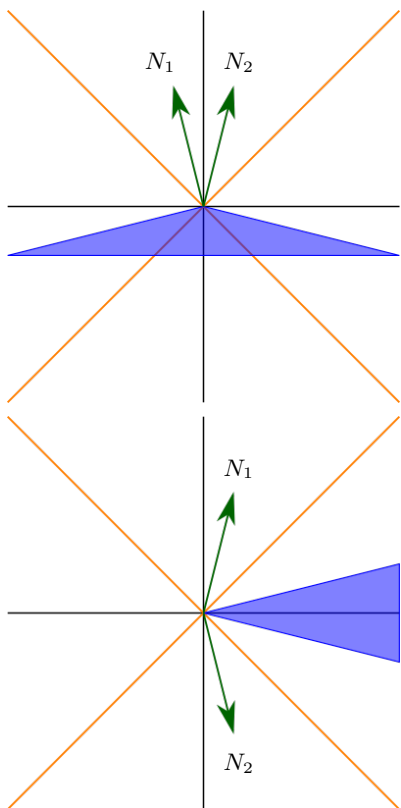


Figure 1: Up: thick wedge, co-chronal normals.
Down: thin wedge, anti-chronal normals.

tion provides an orientation of the wedges. However this orientation does not extend to triangles because several wedges of the same triangle may not have the same orientation.

This notion translates easily on the dual complex. A pair of a face and a vertex (f, v) with $f \in v$ defines a (dual) wedge on the 2-skeleton Δ_2^* . There exists two unique edges e_1 and e_2 such that $e_1, e_2 \in f$ and $e_1, e_2 \in v$. The wedge is *thick* if e_1 and e_2 are both incoming or both outgoing. It is *thin* otherwise.

Algebraically, the wedge orientation can be defined as

$$\varepsilon_v(f) \stackrel{\text{def}}{=} \begin{cases} +\eta & \text{if thick} \\ -\eta & \text{if thin.} \end{cases} \quad (11)$$

It is then easy to show that

$$\varepsilon_v(f) = \eta \varepsilon_v(e_1) \varepsilon_v(e_2). \quad (12)$$

As we have presented it, the wedge orientation is a byproduct of the edge orientation. However, one can wonder whether it possible to go the other way around and to compute the $\varepsilon_v(e)$ as a function of the $\varepsilon_v(f)$, i.e. to invert equation (12)? The short answer is *no*, but not much information is actually missing to do this inversion.

Around the same vertex v , equation (12) defines a system of 10 equations (one per face) with 5 unknowns (one per edge), so we may fear it to be over-constrained. However, the rank of the system (12) is only 4. Indeed, given the orientation $\varepsilon_v(f)$ for any 4 wedges *that do not form a cycle*, one can deduce the orientation of the other 6. Rather than a formal definition, the notion of ‘forming a cycle’ is best understood through few examples on the links of the vertex graph⁷ (see figure 2).

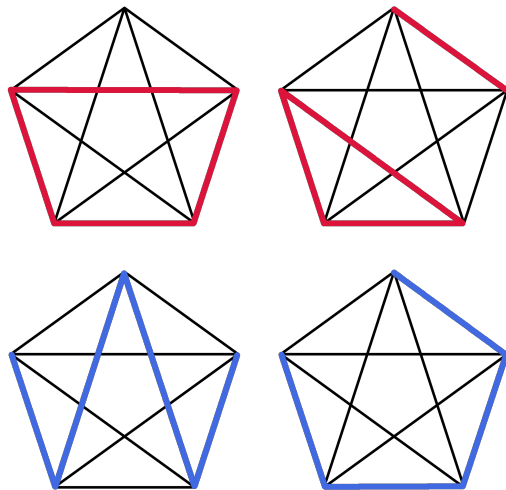


Figure 2: Up: sets of 4 wedges which form cycles.
Down: sets of 4 wedges which do *not* form cycles.

⁷ Given a vertex, the vertex graph associates a node to each edge and a link to each wedge in-between.. In graph theory, the word ‘edge’ is usually used instead of ‘link’. But we stick to a widespread convention in loop quantum gravity (see [2]) where ‘edge’ is reserved to the bulk of 2-complexes and ‘link’ is used for the boundary.

Then it is easy to show that the product of orientations along any cycle of wedges is

$$\prod_{f \in \text{cycle}} \varepsilon_v(f) = \eta^{\#F}, \quad (13)$$

where $\#F$ is the number of faces f around the cycle. Since any set of 5 wedges around v contains a cycle, then 4 wedges orientation are indeed sufficient to fix them all. Hence the system (12) is actually under-constrained of exactly one dimension.

Given a vertex v , denote the surrounding edges by e_i , with $i \in \{1, \dots, 5\}$, and accordingly the surrounding faces by f_{ij} . To make the system invertible, let us add one independent equation, by defining the orientation of the vertex v as:

$$\varepsilon_v \stackrel{\text{def}}{=} \prod_j \varepsilon_v(e_j). \quad (14)$$

Then, the set of equations (12) augmented of (14), with unknowns $\varepsilon_v(e)$, is invertible and one can show that

$$\varepsilon_v(e_i) = \varepsilon_v \prod_{k \neq i} \varepsilon_v(f_{ik}). \quad (15)$$

So we see that we can recover the orientation of the edges from the orientation of the wedges, up to a vertex orientation.

Let's now consider a skeleton with many vertices. Can we deduce the orientation of the edges of the 1-skeleton from the orientation on the wedges of the 2-skeleton? From the previous analysis with a single vertex, we know that it will be possible to invert the system of equations if one considers in addition one orientation ε_v per vertex. However, the set of ε_v is itself constrained, because of the gluing condition (8), which now reads

$$\varepsilon_{v_1} \prod_{f|e \in f} \varepsilon_{v_1}(f) = -\varepsilon_{v_2} \prod_{f|e \in f} \varepsilon_{v_2}(f) \quad (16)$$

This constraint eliminates almost all the degrees of freedom introduced by ε_v , so that there remains finally only the freedom to fix the orientation of a single vertex in the whole skeleton. The orientation of all others can be deduced from it and the $\varepsilon_v(f)$. Indeed, assume that you have a 2-skeleton where all the $\varepsilon_v(f)$ have been fixed (satisfying the constraint along cycles). Then, if you fix only one ε_v , the orientation of the edges around v are fixed, and this 'orientation-fixing' will then propagate everywhere else, so the full set of ε_v will ultimately be fixed. Reversing the orientation of one ε_v , will reverse the entire skeleton, which corresponds to the time-reversal symmetry.

We have previously shown that the causal structure of discrete general relativity can be encoded in the dual 1-skeleton with oriented edges. Now we have just seen that the *causal structure of a 2-skeleton* can be described as the assignation of $\varepsilon_v(f)$ to each wedge under the cycle constraint (13) and a global orientation ε , which can be regarded as a global arrow of time.

IV. LORENTZIAN REGGE CALCULUS

Lorentzian Regge action.

So far, we only focused on the kinematical aspects of causality. Now, we will see how causality shows up in the dynamics [4]. Extending the formulae of [17] to the 4-dimensional case, the lorentzian Regge action is a sum over the triangles t :

$$S_R \stackrel{\text{def}}{=} \sum_t A_t \delta_t, \quad (17)$$

with A_t the area of the triangle t , and δ_t the deficit angle defined as a sum over the 4-simplices σ surrounding t :

$$\delta_t \stackrel{\text{def}}{=} \sum_{\sigma|t \in \sigma} \theta_{t\sigma}, \quad (18)$$

with the dihedral angle defined by equation (9). The order of the two sums can be exchanged:

$$S_R = \sum_{\sigma} \sum_{t|t \in \sigma} A_t \theta_{t\sigma}. \quad (19)$$

To derive the equations of motion by variational calculus, one should tell which are the independent variables of which S_R is a function of. In the original Regge calculus, it is shown that if the action is considered as a function of the lengths l_s of the segments s , the resulting equations of motions become Einstein equations in the continuous limit. However, this is not the only possible choice.

First-order Regge calculus.

Barrett has proposed a formulation where the independent variables are both the lengths l_s and the angles $\theta_{t\sigma}$ [18]. This choice of variables mimics the Palatini formulation which takes the metric and the torsion-less connection as primary fields of the Einstein-Hilbert action. Compared to the original Regge calculus, the introduction of $\theta_{t\sigma}$ extends the total number of variables. In order to recover the equations of motion, it is then necessary to add constraints to the action, which is done with a Lagrange multiplier μ_{σ} per each 4-simplex σ . One obtains

$$S[l_s, \theta_{t\sigma}, \mu_{\sigma}] = \sum_{\sigma} \sum_{t|t \in \sigma} A_t(l_s) \theta_{t\sigma} + \sum_{\sigma} \mu_{\sigma} \det \gamma_{\sigma} \quad (20)$$

where γ_{σ} is the 5×5 matrix whose elements are the minkowskian scalar products between the normals to the boundary tetrahedra:

$$[\gamma_{\sigma}]_{ij} = N_i \cdot N_j = \text{sign}(\theta_{ij}) \cosh \theta_{ij}, \quad (21)$$

where N_i is the (unit outward) normal to the i th boundary tetrahedron of σ and θ_{ij} is the dihedral angle between the tetrahedra i and j . The Lagrange multiplier imposes the constraint

$$\det \gamma_{\sigma} = 0 \quad (22)$$

which implements the closure of the normals, i.e.

$$\sum_i V_i N_i = 0, \quad (23)$$

with V_i the volume of the i th tetrahedron.

Causal structure from dynamics.

This choice of variables for the action makes it very clear how causality plays its role in the dynamics. Indeed, the causal structure shows up in the sign of both the lengths l_s and the angles $\theta_{t\sigma}$. However, assuming all tetrahedra to be space-like, the lengths l_s , and so the areas A_t and volumes V_T , are all positive. So causality appears only in the orientation of the wedges, i.e. the sign of $\theta_{t\sigma}$.

Any set of signs of $\theta_{t\sigma}$ does not define an allowed causal structure as it must satisfy the cycle constraint (13). Interestingly, this condition shows up as a corollary of the equations of motion. Indeed the constraint $\det \gamma_\sigma = 0$ implies the existence of a vector v such that $\sum_i \gamma_{ij} v_i = 0$. Then the equation of motion obtained by varying θ_{ij} yields

$$A_t = \kappa_\sigma \mu_\sigma v_i v_j \sinh \theta_{ij} \quad (24)$$

for some $\kappa_\sigma \in \mathbb{R}$ (see [18]). Since $A_t > 0$,

$$\text{sign } \theta_{ij} = \text{sign}(\kappa_\sigma \mu_\sigma) \text{sign } v_i \text{sign } v_j \quad (25)$$

which implies the constraints (13). This shows that the equations of motion impose the structure of the wedges to be causal.

V. CAUSAL PATH INTEGRAL

So far, the analysis was purely classical, although discrete. When going to the quantum regime of gravity, it is reasonable to expect the generic state of the metric field to be a superposition of classical configurations. In particular, there might not be a definite causal structure. Several causal histories may interfere and thus generate in principle observable effects. A theory of quantum gravity should be able to predict these effects through the computation of transition amplitudes between different states of space.

Let's clarify the main ideas by proceeding heuristically, although a precise mathematical formulation may be more difficult to achieve. The standard procedure starts by foliating the space-time manifold into constant-time slices: $\mathcal{M} \cong \Sigma \times \mathbb{R}$. The classical states are 3-metrics h defined over Σ . At the quantum level, the 3-metric is an operator \hat{h} , with eigenstates $|h\rangle$ whose eigenvalues are the classical 3-metrics h . The sum-over-histories approach to quantum gravity proposes to compute the transition amplitude between the state $|h_0\rangle$ at time t_0 and the state $|h_1\rangle$ at time t_1 as a path integral:

$$\langle h_1 | h_0 \rangle = \int [\mathcal{D}g] e^{\frac{i}{\hbar} S[g]}. \quad (26)$$

$[\mathcal{D}g]$ is a measure on the set of 4-metrics g over $\Sigma \times [t_0, t_1]$, such that the restriction of g to the slice $t = t_0$ (resp. $t = t_1$) is h_0 (resp. h_1). $S[g]$ is the Einstein-Hilbert action evaluated on such a metric.

General boundary formulation.

The previous and standard formulation is not ideal because it relies upon a slicing of space-time into constant-time leaves, which may already fix too much structure for a general treatment of causality. Better suited for our purpose is the general boundary formulation developed by Oeckl in [19].

Consider a region of space-time M with boundary Σ . A 4-metric g on M induces a 3-metric h on Σ . The crux of a quantum theory of space-time is the computation of the *metric propagator*:

$$Z_M(h) = \int [\mathcal{D}g] e^{\frac{i}{\hbar} S[g]} \quad (27)$$

where the integral is carried over all the 4-metrics g bounded by h . The standard formulation (equation (26)) is recovered when Σ is made of two disconnected components (past and future).

Regge path integral.

As a way towards the actual computation of the metric propagator, one can discretise the previous formula. Consider a 4-simplicial complex Δ . Its boundary is a 3-simplicial complex Σ . Working with the Regge action, the metric propagator is a function of the length of the segments of Σ , and it reads:

$$\mathcal{A}_\Delta(l_\Sigma) = \int [dl_s] e^{\frac{i}{\hbar} S_R[l_s]}. \quad (28)$$

The integral is done over the lengths l_s of all the segments s in the bulk of Δ . Note that each integral could also be replaced by a sum with a cut-off, in order to ensure a finite value to the propagator, but it does not seem useful in our quest for causality.

Using the first-order Regge calculus, the propagator reads:

$$\begin{aligned} \mathcal{A}_\Delta(l_\Sigma, \theta_\Sigma, \mu_\Sigma) &= \int [dl_s][d\theta_{t\sigma}][d\mu_\sigma] \\ &\times \prod_\sigma e^{\frac{i}{\hbar} (\sum_{t|t \in \sigma} A_t \theta_{t\sigma} + \mu_\sigma \det \gamma_\sigma)}. \end{aligned} \quad (29)$$

The integration over μ_σ can be formally carried over, which gives a δ -function that fixes the constraint:

$$\mathcal{A}_\Delta(l_\Sigma, \theta_\Sigma) = \int [dl_s][d\theta_{t\sigma}] \prod_\sigma \delta(\det \gamma_\sigma) e^{\frac{i}{\hbar} \sum_{t|t \in \sigma} A_t \theta_{t\sigma}}. \quad (30)$$

Causal structure of the boundary.

A causal structure on Δ induces a causal structure on its boundary Σ . It consists in saying for each tetrahedron of the boundary whether it shall be regarded as

future or past. It can be represented on the boundary of the dual 2-skeleton Δ_2^* , which is a 4-valent graph. The induced causal structure consists in assigning a sign to each node, depending on whether the edge attached to it is pointing inside or outside the bulk. Conventionally, we take the sign to be positive for an outward edge (future tetrahedron) and negative for inward edge (past tetrahedron). An example is shown in figure 3. It is important to notice that fixing a causal structure on the boundary does not in general impose a single causal history in the bulk: many different histories may share the same causal boundary.

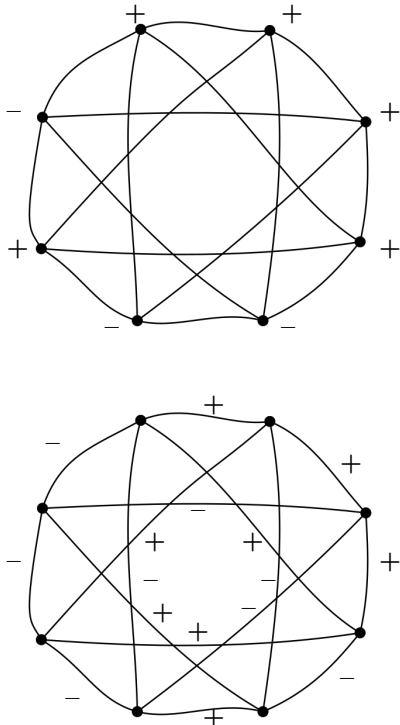


Figure 3: Example of causal structure on a boundary graph. Up: encoded on the nodes. Down: encoded on the links.

The causal information of the boundary can also be encoded on the links. To each link, one associates the product of the sign of the endpoints (see fig. 3). For a 4-valent graph, there are twice as many links as there are nodes. But despite the double number of variables, this encoding is not injective, but 2-to-1. Physically, by encoding causality on the links, we only provide information about bare-causality, while encoding over the nodes also gives a time-orientation.

A random assignment of signs to links only defines a causal structure on the boundary if it enables to consistently assign signs to the nodes. This happens if, and only if, the signs on the links satisfy the constraint that their product around any loop of the graph is 1. The latter constraint is implied by the cycle condition (13) in

the bulk. In fact, when two edges crossing the boundary share a common vertex, the sign of the wedge matches the sign of the link between the two corresponding nodes. More generally, the sign of the link is equal to the product of the signs of the wedges around the corresponding face in the bulk, which can be written

$$\varepsilon_l = \prod_{v \in f} \varepsilon_v(f), \quad (31)$$

where f is the face that intersect the boundary along the link l .

Causal amplitude.

The metric propagator is a function of the boundary variables. In concrete situations, the bare-causal structure of the boundary may be fixed by an assignment of links orientations ε_l . In this case, the range of integration on the angles $\theta_{t\sigma}$ in equation (30) must be restricted for the wedges that belong to faces intersecting the boundary. This restriction consists in implementing the constraint (31). For instance, consider a link l bounding a face f (dual to t) with only one vertex v (dual to σ). If $\varepsilon_l = 1$ (resp. $\varepsilon_l = -1$), then the integration over $\theta_{t\sigma}$ shall be carried over \mathbb{R}^+ (resp. \mathbb{R}^-), instead of \mathbb{R} .

For the $\theta_{t\sigma}$ in the bulk, the integration is still done over all \mathbb{R} . We can rewrite the amplitude (30) as

$$\mathcal{A}_\Delta(l_\Sigma, \eta_\Sigma, \varepsilon_\Sigma) = \sum_{[\varepsilon_{t\sigma}]} \int [dl_s][d\eta_{t\sigma}] \prod_\sigma \delta(\det \gamma_\sigma) e^{\frac{i}{\hbar} \sum_{t|t \in \sigma} A_t \varepsilon_{t\sigma} \eta_{t\sigma}}, \quad (32)$$

where the sum is done over all possible orientations $\varepsilon_{t\sigma}$ of wedges in the bulk, compatible with the bare-causality of the boundary ε_Σ . Thus, the path-integral is also summing over configurations which do not satisfy the cycle condition (13). These configurations have no well-defined causal structure.

However, in the classical limit, when $\hbar \rightarrow 0$, the configurations that contribute the most are the stationary points of the action, which satisfy the classical equations of motion and thus, as seen previously, have a proper causal structure.

It is tempting to implement the causal structure already at the quantum level. By this we mean restricting the sum over the configurations of $\varepsilon_{t\sigma}$ which satisfy the condition (13). Such a strategy is reminiscent of the definition of the Feynman propagator for the relativistic particle. By computing the transition amplitude $\langle x_1 | x_0 \rangle$, with x_0 before x_1 , using the path integral method, one considers only these trajectories which do not go back in time. In this case, the transition amplitude gives the Feynman propagator G_F .

The suggestion of such a causal path-integral for gravity goes back to Teitelboim [20]. In the context of the standard formulation (equation (26)) h_0 is regarded as ‘past’ and h_1 as ‘future’. So Teitelboim proposed to restrict the range of integration over the 4-metrics g to

that which match this time-orientation. When written in the hamiltonian formalism, it amounts to restricting the range of integration of the lapse N to positive values only.

VI. BF THEORY

As a first step towards spin-foams, let's consider discrete BF theory. It is a topological theory, so we do not expect any causal structure to arise, but it makes use of an orientation structure which is worth looking at as a warm-up.

Discrete BF theory.

Following [21], the discretisation of BF theory is done over a 2-complex \mathcal{C} . The variables are one group element $g_e \in G$ per edge $e \in \mathcal{C}$. Then the amplitude is defined as

$$Z_{\mathcal{C}} \stackrel{\text{def}}{=} \int [dg_e] \prod_f \delta(U_f(g_e)). \quad (33)$$

There is one integral per edge, dg_e is the Haar measure over G , δ is the Dirac δ -function over G and the product is carried over all the faces f of \mathcal{C} . Moreover we define the circular product

$$U_f(g_e) \stackrel{\text{def}}{=} \prod_{e \in f}^{\circlearrowleft} g_e, \quad (34)$$

where the product is made over the edges e surrounding f . Although sometimes overlooked, we want to draw attention to the orientation structure which is required to define correctly the circular product. We need the following additional structure over \mathcal{C} :

1. a distinguished edge to each face, that serves as a starting point in the product;
2. an orientation to each face, that tells the order of the following edges.

Although this structure is required to define U_f , $\delta(U_f)$ doesn't actually depends on it, due to the invariance of the δ -function under inversion and cyclic permutation.

It is common to rewrite $Z_{\mathcal{C}}$ by splitting the δ -function into a sum over the irreducible representations (irreps) of G :

$$\delta(U) = \sum_{\rho} \dim \rho \operatorname{Tr} \rho(U) \quad (35)$$

Then, for each edge, the integral over the group element g can be rewritten as a sum over intertwiners, which formally reads

$$\int dg \bigotimes_{f \in e}^{\circlearrowleft} \rho_f(g) = \sum_{\iota} \iota^*. \quad (36)$$

Again, the definition of the circular tensor product requires to introduce additional structure:

3. a distinguished face to each edge, that serves as a starting point in the tensor product;
4. an orientation of the faces around each edge, which can be thought as an arrow on the edge (with the right-hand convention to turn around for instance).

Of course, $Z_{\mathcal{C}}$ remains blind to this structure. The amplitude finally becomes:

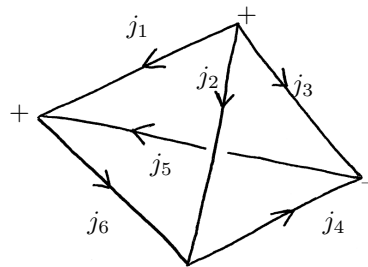
$$Z_{\mathcal{C}} = \sum_{\rho} \sum_{\iota} \prod_f \dim \rho_f \prod_v A_v. \quad (37)$$

The sum in ρ (resp. ι) is made over all the possible labelling of the faces (resp. edges) by irreps (resp. intertwiners). The *vertex amplitude* A_v is a function of the irreps ρ_f and intertwiners ι_e attached to the faces and edges surrounding a vertex v .

The four orientation structures just introduced enter the computation of A_v . These structures lie on the edges and faces of the 2-complex. Motivated by our analysis in the previous sections, we want to investigate the idea that causality of spin-foams could arise from the breaking of the invariance of $Z_{\mathcal{C}}$ with respect to the orientation of \mathcal{C} .

Ponzano-Regge model.

To proceed concretely, let's consider the simple example of the *Ponzano-Regge model* [22], for which \mathcal{C} is dual to a 3-dimensional simplicial complex Δ , and $G = SU(2)$. In this case, the irreps are labelled by spins $j \in \mathbb{N}/2$ and there is no sum over the intertwiners (because it is unique). The vertex amplitude can be nicely represented pictorially as a graph where each node stands for an adjacent edge and each link for a face in-between. The *vertex graph* takes typically the following form:



(38)

The arrows on the links are induced by the orientation of the faces and the signs on the nodes are induced by the orientation of the edges (+ for incoming). Any combination of arrows and signs can be found, but the topology of the graph is the same for every vertex. The labels j on the links are inherited from the irreps on the faces.

The graphical calculus is defined with the following rules:

1. To each link l , associate a variable m_l that will be summed over;

2. The $3jm$ -Wigner symbol⁸ is associated to the following nodes:

$$\begin{aligned} \begin{pmatrix} j_1 & j_2 & j_3 \\ m_1 & m_2 & m_3 \end{pmatrix} &= \begin{array}{c} \begin{array}{ccc} & \nearrow^{j_2} & \\ \nwarrow^{j_3} & \downarrow & \nearrow^{j_1} \\ & + & \end{array} \\ \\ = \begin{array}{c} \begin{array}{ccc} & \nwarrow^{j_2} & \\ \nwarrow^{j_1} & \downarrow & \nwarrow^{j_3} \\ & - & \end{array} \end{array} \end{array} \quad (39) \end{aligned}$$

The sign on the node indicates the sense in which the attached links shall be read.

3. If an arrow is reversed, replace in the formula above m_l by $-m_l$ and multiply by $(-1)^{j_l - m_l}$, like

$$\begin{array}{c} \begin{array}{ccc} & \nearrow^{j_2} & \\ \nwarrow^{j_3} & \downarrow & \nearrow^{j_1} \\ & + & \end{array} \\ \text{or} \end{array} = (-1)^{j_3 - m_3} \begin{pmatrix} j_1 & j_2 & j_3 \\ m_1 & m_2 & -m_3 \end{pmatrix} \quad (40)$$

$$\begin{array}{c} \begin{array}{ccc} & \nwarrow^{j_2} & \\ \nwarrow^{j_1} & \downarrow & \nwarrow^{j_3} \\ & - & \end{array} \end{array} = (-1)^{j_1 - m_1} \begin{pmatrix} j_1 & j_2 & j_3 \\ -m_1 & m_2 & m_3 \end{pmatrix} \quad (41)$$

A positive (resp. negative) node with an incoming (resp. outgoing) link corresponds to a counter-alignment of the face and the edge.

4. Multiply all factors and sum over all m_l from $-j_l$ to j_l (integer steps).

As an example, the graph (38) evaluates to

$$\begin{aligned} A_v &= \sum_{m_i} (-1)^{j_4 - m_4 + j_1 - m_1} \begin{pmatrix} j_1 & j_2 & j_3 \\ m_1 & m_2 & m_3 \end{pmatrix} \\ &\times \begin{pmatrix} j_4 & j_5 & j_3 \\ m_4 & -m_5 & m_3 \end{pmatrix} \begin{pmatrix} j_6 & j_2 & j_4 \\ m_6 & m_2 & -m_4 \end{pmatrix} \begin{pmatrix} j_6 & j_5 & j_1 \\ m_6 & -m_5 & -m_1 \end{pmatrix} \end{aligned} \quad (42)$$

The power of graphical calculus is apparent when comparing this cumbersome formula to the diagram (38). Up to a sign, the vertex amplitude equals the $6j$ -symbol:

$$A_v = \pm \left\{ \begin{array}{ccc} j_1 & j_2 & j_3 \\ j_4 & j_5 & j_6 \end{array} \right\}. \quad (43)$$

The sign \pm is a function of the spins j_i and it depends on the orientation of the links and nodes. It matters when several vertices are glued together.

The importance of the Ponzano-Regge model is revealed by its semi-classical limit, which makes it a good candidate for 3D euclidean quantum gravity [22]. Indeed, the vertex amplitude admits a graphical representation as a tetrahedron depicted in (38). This shape initially expresses the invariance of the $6j$ -symbol under the action of the tetrahedral group. But it turns out that it also carries a deeper geometric meaning when the labels j_i are interpreted as the edge lengths of the tetrahedron. Denoting V the volume of this tetrahedron, one can prove the following behaviour for the vertex amplitude $A_v(\lambda j_i)$ when $\lambda \rightarrow \infty$:

$$\left\{ \begin{array}{ccc} \lambda j_1 & \lambda j_2 & \lambda j_3 \\ \lambda j_4 & \lambda j_5 & \lambda j_6 \end{array} \right\} \sim \frac{1}{4\sqrt{3\pi\lambda^3 V}} (e^{iS} + e^{-iS}) \quad (44)$$

with the action

$$S \stackrel{\text{def}}{=} \sum_i \left(\lambda j_i + \frac{1}{2} \right) \xi_i + \frac{\pi}{4} \quad (45)$$

with ξ_i the exterior dihedral angle along the edge i [24].

Graphical calculus also clarifies how the orientation enters the computation of the vertex amplitude. The invariance of the total amplitude $Z_{\mathcal{C}}$ under changes of orientation of the edges and faces is checked in appendix A. To be precise, the invariance is only true for faces and edges which lie in the bulk of \mathcal{C} . In general, \mathcal{C} is bounded by some 3-valent graph Γ over which an orientation is induced by \mathcal{C} . The total amplitude $Z_{\mathcal{C}}$ is sensitive to the orientation of Γ . The case is similar to the amplitude defined by equation (32). Although topological in the bulk, BF theory is non-trivial on the boundary. The boundary orientation provides a prototype of boundary causal structure.

A change of boundary orientation affects the value of $Z_{\mathcal{C}}$ in a simple way:

- A flip of a link-orientation brings a global factor $(-1)^{2j}$ if the two-endpoints carry opposite signs, none otherwise.
- A flip of a node-orientation brings an overall factor $(-1)^{j_1 + j_2 + j_3}$.

As for Feynman diagrams, this simple way of modifying the causal structure of the boundary can be understood as a *crossing symmetry*.

Causal Ponzano-Regge model.

Now we want to go further and suggest a way to break the orientation-invariance in the bulk of the Ponzano-Regge model.

Consider \mathcal{H}_j , the spin- j irreducible representation of $SU(2)$, with the canonical basis $|jm\rangle$. The coherent states are defined as

$$|j, z\rangle \stackrel{\text{def}}{=} u(z) |j, -j\rangle \quad (46)$$

⁸ We refer to [23] for an introduction to the mathematical material used in this section.

with $u : \mathbb{C}^2 \rightarrow SU(2)$ a (well-chosen) surjective map. Then, the intertwiner can be written as the state

$$|\iota\rangle = \frac{1}{N} \int dg g \cdot \bigotimes_{i=1}^3 |j_i, z_i\rangle \quad (47)$$

with $N = N(j_i, z_i)$ such that $\langle \iota | \iota \rangle = 1$. Up to a global phase, the vertex amplitude is

$$A_v = \frac{1}{N} \int_{SU(2)} [dg_n] \prod_l K_l(g_{t_l}, g_{s_l}). \quad (48)$$

t_l and s_l are respectively the source and the target of l . The wedge amplitude is defined as

$$K(g_t, g_s) \stackrel{\text{def}}{=} \langle j, z_t | g_t^{-1} g_s | j, z_s \rangle = \langle z_t | g_t^{-1} g_s | z_s \rangle^{2j}. \quad (49)$$

For the purpose of studying the semi-classical limit, it is convenient to write the wedge amplitude as

$$K(g_t, g_s) = e^{2j(\log r + i\theta)} \quad (50)$$

with $r \in \mathbb{R}^+$ and $\theta \in (-\pi, \pi]$.

Now, to introduce a notion of causality, we can force some orientation structure to appear artificially: this is done here by writing the identity

$$K(g_t, g_s) = \sum_{\varepsilon \in \{1, -1\}} \Theta(\varepsilon\theta) e^{2j(\log r + i\varepsilon\theta)}, \quad (51)$$

where Θ is the step function and we are summing over the signs ε . We then define the causal wedge amplitude as

$$K^\varepsilon(g_t, g_s) \stackrel{\text{def}}{=} \Theta(\varepsilon\theta) e^{2j(\log r + i\varepsilon\theta)}. \quad (52)$$

for some choice of ε , which can be understood as a choice of wedge orientation. Given one orientation ε_l per wedge l , the causal vertex amplitude A_v^ε is defined by replacing the wedge amplitude K_l by its causal alternative $K_l^{\varepsilon_l}$ in equation (48). The BF vertex amplitude is recovered as

$$A_v = \sum_{[\varepsilon_l]} A_v^{\varepsilon_l}, \quad (53)$$

where the sum is made over all possible sign-assignment to the wedges. There is a total of 2^6 such configurations. This sum introduces a partition of the range of integration of (48) into as many sectors. In the semi-classical limit, only two sectors survive, as it appears in (44). Since the exterior dihedral angles of any tetrahedron are always such that $\sin \xi \leq 0$, the two sectors are when ε_l are either all positive or all negative. Starting with the causal vertex amplitude with all ε_l negative thus leads to the asymptotic limit

$$A_v^- \sim \frac{1}{4\sqrt{3\pi V}} e^{iS}. \quad (54)$$

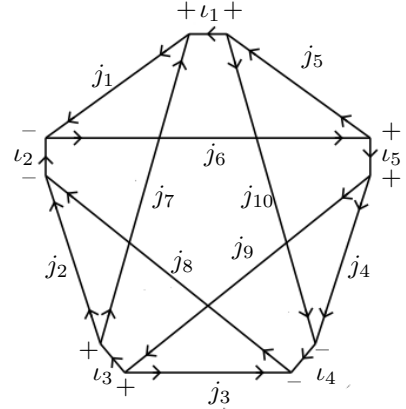
This provides a toy-model for the appearance of causality, which we will apply to the EPRL model.

{15j} BF theory.

Before moving to the EPRL model, let us look at BF theory in 4 dimensions. The main difference with respect to the $3d$ case comes from the fact that Δ is a 4-dimensional simplicial complex and so the amplitude Z_C includes a sum over the intertwiners. The graphical representation of the intertwiners requires the introduction of an additional structure:

5. at each edge, the surrounding faces are partitioned into two sets of two (there exists three such partitions);
6. these two sets are ordered (e.g. called left and right).

Then the vertex amplitude is represented by a pentagram like



(55)

$\iota \in \mathbb{N}/2$ is labelling the intertwiners. It is surrounded by two positive (resp. negative) nodes, when the edge is incoming (resp. outgoing). When the nodes are positive (resp. negative), the arrow goes from the right set to the left set (resp. the other way around). One can check with the rules above, that the overall amplitude Z_C is insensitive to the additional structure introduced. The same procedure as before can be used to define the causal vertex amplitude A_v^ε .

To sum up, discrete BF theory is defined over a 2-complex \mathcal{C} with a bunch of auxiliary orientation structures. The value of the partition function Z_C is sensitive to the boundary values of these structures, but not in the bulk. However, we have made a proposal to select a causal structure in the bulk as well.

VII. EPRL MODEL

General relativity can be formulated in a language close to the one of BF theory. The essential difference is that GR has local degrees of freedom, which mathematically arise from the implementation of constraints on the BF variables. Spin-foam models build upon this

insight and consist in a weak implementation of these constraints in the discrete BF theory.

The appearance of the local degrees of freedom shows up in the breaking of the topological invariance of BF theory. The question then arises if these constraints induce also a causal structure on the 2-complex. The analysis of the previous sections suggests that such a causal structure can arise as an orientation structure on the edges or the wedges. Imposing constraints on these orientations then breaks the bulk orientation invariance of BF theory discussed above. In this section, we propose such a construction for the EPRL model.

Lorentzian EPRL model.

The EPRL model [5], as formulated in [25], is defined over a 2-complex \mathcal{C} by the following partition function:

$$Z_{\mathcal{C}} = \int_{SU(2)} [dh_w] \prod_f \delta(U_f) \prod_v A_v(h_w). \quad (56)$$

The integral is made over the variables $h_w \in SU(2)$ associated to each wedge w in the bulk of \mathcal{C} . $Z_{\mathcal{C}}$ is a function of the variables $h_l \in SU(2)$ associated to each link of the boundary graph Γ . Similarly to BF theory, the precise definition requires additional structure on Γ :

1. a starting wedge per each face;
2. an orientation per each face;
3. an orientation to each wedge, i.e. each wedge w has a source edge s_w and a target edge t_w ;
4. a distinguished edge E_v per each vertex v .

Then, U_f is defined as the circular product

$$U_f(h_w) \stackrel{\text{def}}{=} \prod_{w \in f}^{\circlearrowleft} h_w \quad (57)$$

that starts with the starting wedge of f , circulates in the sense given by the orientation of f , and each h_w is inverted when the orientation of the wedge does not match with the orientation of the face. Besides, the vertex amplitude is

$$A_v(h_w) = \int_{SL_2(\mathbb{C})} [dg_e] \delta(g_{E_v}) \prod_{w \in v} K(h_w, g_{s_w} g_{t_w}^{-1}) \quad (58)$$

where there is one integration over $SL_2(\mathbb{C})$ per each edge surrounding v . The $\delta(g_{E_v})$ is only here to make the integral finite, but the value of A_v is actually independent on the choice of E_v . The wedge amplitude K is a function over $SU(2) \times SL_2(\mathbb{C})$ given by

$$K(h, g) = \sum_j (2j+1)^2 \int_{SU(2)} dk \overline{\chi^j(hk)} \chi^{\gamma j, j}(kg), \quad (59)$$

with χ^j and $\chi^{p, k}$ respectively the characters of $SU(2)$ and $SL_2(\mathbb{C})$, and $\gamma \in \mathbb{R}$ the Barbero-Immirzi parameter.

The success of the EPRL model lies in its semi-classical limit, which was studied in [10, 26] for a 2-complex \mathcal{C} made of a single vertex dual to a lorentzian 4-simplex σ . In this case, the partition function reduces to a single vertex amplitude $A_v(h_w)$, function of one $SU(2)$ element h_w per each of the 10 links of the boundary graph. The boundary of σ is made of 5 tetrahedra which can be described by the areas j and the normals \vec{n} to their faces. Then, the kinematics of loop quantum gravity prescribes a construction of a coherent state $\Psi_{j, \vec{n}}(h_w)$ which is ‘peaked’ on the boundary geometry of σ . In the limit of large areas, $\lambda \rightarrow \infty$,

$$\begin{aligned} \langle \Psi_{\lambda j, \vec{n}} | A_v \rangle &\stackrel{\text{def}}{=} \int_{SU(2)} [dh_w] \Psi_{j, \vec{n}}^*(h_w) A_v(h_w) \\ &\sim \frac{1}{\lambda^{12}} (N_{\sigma} e^{i\lambda S_R} + N_{P\sigma} e^{-i\lambda S_R}) \end{aligned} \quad (60)$$

with $N_{\sigma}, N_{P\sigma} \in \mathbb{R}$ and S_R is the lorentzian Regge action of σ . This result is encouraging because it is close to the classical expectation and takes the same form (44) for the semiclassical limit of the Ponzano-Regge model. However, it is not without flaws as we will discuss later.

The EPRL model is blind to the bulk orientation structure that has been introduced to define it. Indeed, changing the starting wedge or the orientation of a face f changes the value of U_f but not of $\delta(U_f)$. Moreover, reversing the orientation of a wedge w changes both U_f and A_v . In U_f it replaces h_w by h_w^{-1} . In A_v , it interchanges s_w and t_w , and so $K(h_w, g_{s_w} g_{t_w}^{-1})$ becomes $K(h_w, g_{t_w} g_{s_w}^{-1})$, which is easily shown to be equal to $K(h_w^{-1}, g_{s_w} g_{t_w}^{-1})$. A change of variables $h_w \rightarrow h_w^{-1}$ within the integral finally proves that the value of $Z_{\mathcal{C}}$ remains unchanged.

The model is nevertheless sensitive to the orientation structure on the boundary. This structure consists only of the orientation of the links on the boundary over which the variables h_l live. In the light of our preceding analysis, we expect this structure to carry causal information.

Causal EPRL model.

Analogously to our previous toy-model for BF theory, one can break the orientation invariance in the bulk as follows. First, one performs the integral over $k \in SU(2)$ in (59), which yields

$$K(h, g) = \sum_{j, m, n} (2j+1) \overline{D_{mn}^j(h)} D_{jm, jn}^{\gamma j, j}(g). \quad (61)$$

One can switch from the magnetic basis $|jm\rangle$ to the overcomplete coherent states basis $|j, z\rangle$, by introducing a resolution of the identity

$$\mathbb{1}_j = \frac{2j+1}{\pi} \int_{\Gamma} \frac{\Omega(z)}{\|z\|^4} |j, z\rangle \langle j, z| \quad (62)$$

with the measure

$$\Omega(z) \stackrel{\text{def}}{=} \frac{i}{2} (z_0 dz_1 - z_1 dz_0) \wedge (z_0^* dz_1^* - z_1^* dz_0^*). \quad (63)$$

Here Γ is the image of a path $\mathbb{C}P^1 \rightarrow \mathbb{C}^2$ that crosses each vector line of \mathbb{C}^2 once and only once⁹. One gets

$$K(h, g) = \sum_j \frac{(2j+1)^3}{\pi^2} \int_{\Gamma' \times \Gamma''} \frac{\Omega(z')\Omega(z'')}{\|z'\|^4 \|z''\|^4} \times \langle j, z' | h^\dagger | j, z'' \rangle \langle \gamma j, j, j, z'' | D^{\gamma j, j}(g) | \gamma j, j, j, z' \rangle. \quad (64)$$

Following [10, 26], the $SL_2(\mathbb{C})$ matrix element appearing above can be expressed in terms of an auxiliary $\mathbb{C}P^1$ as

$$\langle \gamma j, j, j, z'' | D^{\gamma j, j}(g) | \gamma j, j, j, z' \rangle = \frac{2j+1}{\pi} \int_{\Gamma} \frac{\Omega(\zeta)}{\|\zeta\|^4} \mathcal{A} e^{iS_\gamma}, \quad (65)$$

where

$$\mathcal{A} = \frac{\langle \zeta | z''^* \rangle^{2j} \langle z'^* | g^T \zeta \rangle^{2j} e^{2ij(\arg z'' - \arg z')}}{\|z'\|^{2j} \|z''\|^{2j} \|\zeta\|^{2j-2} \|g^T \zeta\|^{2j+2}} \quad (66)$$

and

$$S_\gamma = \gamma j \log \frac{\|g^T \zeta\|^2}{\|\zeta\|^2}. \quad (67)$$

One can thus define the causal wedge amplitude as

$$K_\varepsilon(h, g) = \sum_j \frac{(2j+1)^4}{\pi^3} \int \frac{\Omega(\zeta)\Omega(z')\Omega(z'')}{\|\zeta\|^4 \|z'\|^4 \|z''\|^4} \times \langle z' | h^\dagger | z'' \rangle^{2j} \Theta(\varepsilon S_\gamma) \mathcal{A} e^{iS_\gamma}. \quad (68)$$

The causal vertex amplitude A_v^ε is then defined by replacing K with K_ε in equation (58), for some choice of ε on each wedge. This defines a causal EPRL model.

At this level, the epithet ‘causal’ is only motivated by the fact that the extra variable $\varepsilon \in \{1, -1\}$ can potentially encode a causal structure on the wedges, as described previously. Let’s motivate it further.

First, the usual vertex amplitude is recovered by summing over all possible sign-assignment to wedges:

$$A_v = \sum_{[\varepsilon_w]} A_v^\varepsilon. \quad (69)$$

There are 2^{10} terms in the sum. If one interprets ε as wedge orientations, then a configuration only properly defines a causal structure if the cycle condition (13) is fulfilled. So, one can properly call A_v^ε a ‘causal vertex amplitude’ when the configuration $[\varepsilon_w]$ satisfies (13).

Secondly, assuming that the $[\varepsilon_w]$ indeed defines a proper causal structure, the word ‘causal’ for A_v^ε is only deserved if, in the asymptotic limit, ε really captures the causal orientation of the boundary state. More precisely, given a lorentzian 4-simplex, it determines a set of $\tilde{\varepsilon}$ for

each wedge, such that $\tilde{\varepsilon}_w = \text{sign } \theta_w$, where θ_w is the dihedral angle of the wedge w . Then, its boundary coherent state $\Psi_{j, \vec{n}}$, when contracted with A_v^ε , should have the expected classical limit, i.e.

$$\langle \Psi_{\lambda j, \vec{n}} | A_v^\varepsilon \rangle \sim \frac{1}{\lambda^{12}} N_\sigma e^{i\lambda S_R} \quad (70)$$

One can check that this is the case. Indeed, $\langle \Psi_{\lambda j, \vec{n}} | A_v \rangle$ is an integral over the variables g, z, z' . The sum (69) introduces a partition of the range of integration in a number of sectors $[\varepsilon_w]$ characterised by $\varepsilon_w S_\gamma(x_w) > 0$, where x_w stands for all the variables g, z, z' on the wedge w . In the asymptotic limit, the two terms of (60) arise from two stationary points which are related by a parity transformation. The asymptotic analysis of [27] shows that one of them, denoted σ , is such that $\tilde{\varepsilon}_w S_\gamma(x_w^\sigma) > 0$. Then the other, denoted $P\sigma$, satisfies $S_\gamma(x_w^{P\sigma}) = -S_\gamma(x_w^\sigma)$, so that $P\sigma$ and σ are in opposite sectors. By construction, $\langle \Psi_{\lambda j, \vec{n}} | A_v^\varepsilon \rangle$ selects only the sector of σ .

The asymptotic behaviour (70) is the only criterion that constrains the definition of the causal wedge amplitude. So, the dichotomy operated by $\Theta(\varepsilon S_\gamma)$ is to some extent arbitrary, and other functions could work as well. Another choice of K_ε would define a different quantum theory with the same classical limit. Our choice appears to us as the simplest one. Its technical properties will be discussed in a second article.

The causal EPRL model is not a new model, but rather an interpretation of different components of the standard vertex amplitude in terms of causal structures. This interpretation is motivated *a priori* by the understanding that discrete causal structures can be encoded on wedges, and *a posteriori* by the asymptotics of the causal vertex. In the next section, we discuss how the proposal connects to earlier results, and this motivates the idea that taking causality into account could cure some of the EPRL model’s known issues.

VIII. RELATION TO EARLIER PROPOSALS

Livine-Oriti Barrett-Crane causal model.

Our approach is closely related to an earlier proposal on the implementation of causality by Livine and Oriti [6]. In the context of the Barrett-Crane model, the wedge amplitude is

$$K^p(x_1, x_2) = \frac{2 \sin(\beta(x_1, x_2) p/2)}{p \sinh \beta(x_1, x_2)}. \quad (71)$$

x_1 and x_2 can be understood as the normals to two boundary tetrahedra and $\beta(x_1, x_2)$ is the lorentzian angle in-between (see appendix B for a complete definition of the symbols). The Livine-Oriti proposal consists in expanding the sine as

$$K^p(x_1, x_2) = \frac{1}{p \sinh \beta(x_1, x_2)} \sum_{\varepsilon = \pm 1} \varepsilon e^{i\varepsilon \beta(x_1, x_2) p/2}, \quad (72)$$

⁹ More abstractly, it can be regarded as a section of the Hopf bundle.

interpreting ε as an orientation on the wedges and selecting one of the two sectors only. The implementation of causality discussed in this paper can be understood as a direct generalization of the Livine-Oriti proposal to the EPRL model. The non-trivial step introduced here is in the identification of how to introduce the splitting in (68).

Divergence and spikes.

The EPRL model and the Ponzano-Regge model both suffer from infrared divergences. In the latter case, the simplest example is provided by a triangulation Δ made of four tetrahedra subdividing a bigger tetrahedron. The dual 2-complex has 4 vertices and 10 faces. The four interior faces enclose a *bubble*. The partition function is given by

$$Z_C = \sum_{j_i} \left(\prod_f (2j_f + 1) \right) A_{v_1} A_{v_2} A_{v_3} A_{v_4}. \quad (73)$$

The sum is made over the spins j_i attached to the interior faces. The spins of the other faces are not summed over because they are fixed by the boundary conditions. The range of the sum for each interior face is a priori restricted by its neighboring faces according to the Clebsh-Gordan conditions. But the existence of a bubble implies that the sums are actually unbounded. This wouldn't be a problem if the vertex amplitude A_v was decreasing fast enough for large spins, but such is not the case.

In the asymptotic limit, A_v consists of two conjugate terms like

$$A_v \sim A_v^+ + A_v^-, \quad (74)$$

as shown in equation (44). The sign \pm can be seen as an orientation of the tetrahedron dual to v . Thus,

$$A_{v_1} A_{v_2} A_{v_3} A_{v_4} \sim \sum_{\varepsilon_i} A_{v_1}^{\varepsilon_1} A_{v_2}^{\varepsilon_2} A_{v_3}^{\varepsilon_3} A_{v_4}^{\varepsilon_4}, \quad (75)$$

where the sum is carried over all possible sign-assignment to the four vertices. In [28], it is suggested that only some of the terms in this sum, dubbed 'spikes', contribute to the divergence. In other words, a wise selection of vertex orientation can cure the model from divergences. It is suggested that a similar behavior could cure the EPRL model as well.

Our proposed causal EPRL model (68) satisfies the requirements identified in [28]. However, there are two main differences with respect to their proposal:

1. We fix the orientation at the level of wedges, which is a finer scale than that of tetrahedra.
2. The orientation is fixed in the definition of the amplitude, while theirs only holds in the asymptotic limit.

Engle's proper vertex.

The computation of the EPRL asymptotics (60) by Barrett et al [27] is promising but presents two difficulties:

- The cosine problem: the asymptotics of a single vertex has two critical points. This results in a problematic asymptotic behavior when several vertices are involved.
- Euclidean boundary: the asymptotics does not suppress the euclidean boundary.

These two difficulties are traced back to a common origin in Engle's analysis [7, 8]: the EPRL model is built from discrete BF theory by imposing the simplicity constraint, but the latter is not strong enough as it admits three sectors out of the five of the Plebanski formulation.

The *proper vertex* [8] includes further constraints that restrict the model to the Einstein-Hilbert sector only. This is done by introducing in each wedge amplitude a spectral projector that concretely acts as a step-function Θ . As a result, only one of the two terms in (60) is selected.

Our proposed causal vertex (68) shares a similar feature in that it amounts to the introduction of a step-function on each wedge. Yet, let us remark that:

1. The motivations are different. Engle's proper vertex is motivated by the restriction to the Einstein-Hilbert sectors while we are motivated by our analysis of the causal structure. Do the two requirements actually coincide? It would be interesting to investigate this relation, following the analysis of Immirzi in [16].
2. A priori, it is not clear that the two restrictions match away from the semi-classical limit. In fact, Engle's proper vertex introduces a step-function Θ on each wedge which depends on data on the full 4-simplex, while (68) is local on the wedge but includes the wedge orientations ε_w as additional dynamical variables.

IX. CONCLUSION

We can summarise our main points as follows:

- The notion of causality in general relativity encompasses two related but conceptually different notions: bare-causality and time-orientability.
- There is a natural way to translate these notions to a simplicial complex.
- The causal structure can be implemented on the dual 1-skeleton (edges). It can be seen as the combination of a causal set with a neighbourhood relation.

- It can also be encoded on the dual 2-skeleton (wedges) with a degeneracy of 2 that corresponds to a global time-reversal symmetry.
- Starting from the set of all possible wedge orientations, the lorentzian Regge action determine equations of motion whose solutions fix a proper causal structure.
- The metric propagator can be written as a sum over all possible wedge orientations. By fixing the causal structure from the beginning, one defines a causal metric propagator, similar to the Feynman propagator.
- The discrete BF theory naturally carries an orientation structure on the edges and faces, although it is blind to it in the bulk.
- The discrete BF theory is sensitive to the orientation on the boundary. There are simple rules of crossing symmetry to go from one orientation to another
- There is an easy way to break the orientation invariance in the bulk, which provides a toy-model to study causality in spin-foam models.
- The EPRL amplitude can be regarded as a sum over all possible configurations of wedge orientations ε_w , which provide additional dynamical variables encoding the causal structure. Only a subset of it corresponds to properly causal configurations.
- The causal EPRL vertex shares common traits with the Livine-Oriti causal version of the Barrett-Crane model and with Engle's proper vertex. It cures some of the flaws of the initial model.
- The causal EPRL model shows a new form of rigidity: only discrete lorentzian geometries compatible with the fixed causal structure arise in the semiclassical limit. This phenomenon provides an analogue of Malament's theorem for semiclassical spinfoams.

Acknowledgments

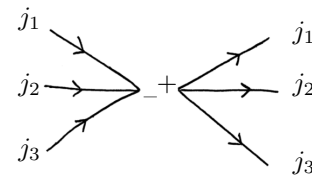
The authors thank Pietro Donà and Francesco Gozzini for insights and constructive criticisms during the course of this work. PMD thanks Alexandra Elbakyan for her help to access the scientific literature.

This publication was made possible through the support of the ID# 61466 grant from the John Templeton Foundation, as part of the "Quantum Information Structure of Spacetime (QISS)" project (qiss.fr). The opinions expressed in this publication are those of the authors and do not necessarily reflect the views of the John Templeton Foundation. EB acknowledges support by the NSF via the Grant PHY-1806428.

Appendix A: Orientation invariance of Ponzano-Regge model

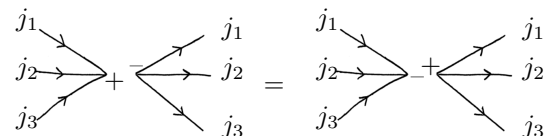
The Ponzano-Regge model is defined over a 2-complex \mathcal{C} . To write the partition function like (37), it is necessary to introduce an orientation structure on the edges and faces. However, the value of $Z_{\mathcal{C}}$ is independent of this structure in the bulk. This can be checked as follows.

Consider an edge. Its orientation plays a role in the amplitudes of the two vertices that terminates the edge. Graphically, the contribution of the edge is



$$(A1)$$

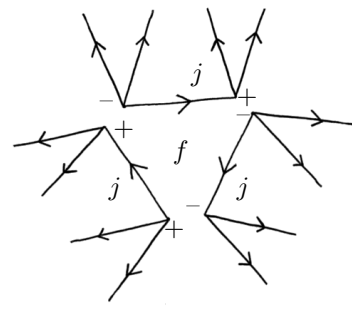
The face orientation, represented by the arrows, is actually irrelevant to the property that we are proving. What matters is that an edge spawns two nodes, one positive and one negative. Reversing the orientation amount to switching the signs of both nodes. With the above rules, it is easy to check that



$$(A2)$$

which proves the invariance under change of edge-orientation.

Now consider a face. Its orientation plays a role in the amplitudes of all the vertices around the face. For instance, in the case of a face labelled by j and surrounded by three vertices, its orientation appears as an arrow on the j -link of three vertex amplitudes, like



$$(A3)$$

Reversing the orientation of the face amounts to reversing the arrow on each of the links around. Now, using the above rules, it is easy to show that

1. Reversing the arrow of a link in-between two positive or two negative nodes, amounts to multiplying by $(-1)^{2j}$.
2. Reversing the arrow of a link in-between a positive and a negative link does not change the vertex amplitude.

So overall, one gets a factor $(-1)^{2j}$ for each link surrounded by nodes of the same sign. To conclude, we need to prove the lemma that the number of such links around a face is always even. Indeed, choose a face and call V is the number of vertices around, and D (resp. S) is the number of links around that have endpoint nodes with different (resp. the same) signs. We have $S + D = V$. Then notice that there are in total as many positive as negative nodes, so that the product of the signs of the nodes around a face is $(-1)^V$. The same quantity can be computed differently as $(-1)^D$. This shows that V and D have the same parity, which implies that S is even and proves the lemma. As a conclusion, Z_C is indeed invariant under a change of face-orientation.

Appendix B: Causal Barrett-Crane model

In this appendix, we review the Livine-Oriti causal version of the lorentzian Barrett-Crane spin-foam [6].

Lorentzian Barrett-Crane.

The lorentzian Barrett-Crane model was introduced in [29]. The 2-complex \mathcal{C} is dual to a 4-dimensional simplicial complex Δ and each face f is labelled by a positive number $p_f \in \mathbb{R}_+$. As formulated in [6]¹⁰, the partition function reads

$$Z_C = \int_{\mathbb{R}^+} [dp_f] \prod_f p_f^2 \prod_e A_e \prod_v A_v. \quad (\text{B1})$$

The integral is carried over the labels p_f for each face. The edge amplitude is given by

$$A_e = \int_{(H^+)^2} dx_1 dx_2 \prod_{f \in e} K^{p_f}(x_1, x_2). \quad (\text{B2})$$

The integration is carried over variables $x_1, x_2 \in H^+$ of the upper hyperboloid and the so-called kernel

$$K^p(x_1, x_2) = \frac{2 \sin(\beta(x_1, x_2) p/2)}{p \sinh \beta(x_1, x_2)} \quad (\text{B3})$$

with $\beta(x_1, x_2)$ the lorentzian angle between x_1 and x_2 :

$$\beta(x_1, x_2) \stackrel{\text{def}}{=} \cosh^{-1}(x_1 \cdot x_2) \geq 0. \quad (\text{B4})$$

Surrounding a vertex v , the edges are labelled with an index $i \in \{1, \dots, 5\}$, and the faces are consistently labelled

by a couple of such indices. Then the vertex amplitude is computed as

$$A_v = \int_{(\mathcal{H}^+)^5} [dx_e] \delta(x_5 - 1) \prod_{(ij)} K^{p_{ij}}(x_i, x_j). \quad (\text{B5})$$

It is striking to realise that the formulae are expressed without any reference to the orientation of \mathcal{C} . In this sense, the lorentzian Barrett-Crane model is completely blind to the causal structure to the extent that it does not even take care of the causal structure on the boundary.

Livine-Oriti causal model.

The latter fact was recognised has unsatisfactory by Livine and Oriti in [6]. Rewriting the kernel as

$$K^p(x_1, x_2) = \frac{1}{p \sinh \beta(x_1, x_2)} \sum_{\varepsilon = \pm 1} \varepsilon e^{i\varepsilon \beta(x_1, x_2) p/2} \quad (\text{B6})$$

we see that the lorentzian Barrett-Crane gives the amplitude:

$$Z(\Delta) = \sum_{\varepsilon_f} \int_{(\mathcal{H}^+)^5} [dx_e] \delta(x_5 - 1) \left(\prod_{f \in v} \frac{\varepsilon_f}{p_f \sinh \beta_f} \right) e^{i \sum_f \varepsilon_f \beta_f p_f/2}. \quad (\text{B7})$$

where the sum is carried over all possible sign assignation to the faces f around the vertex v . The p_f are related to the area of the boundary triangle by

$$p_f = \lambda A_f. \quad (\text{B8})$$

In the semi-classical limit, when $\lambda \rightarrow \infty$, the sum over ε_f and the integral over x_e in (B7) are dominated by only two terms for which the variables describe the two only possible 4-simplices which have p_f as areas up to degenerate contributions.

The coexistence of two terms in the asymptotic limit can be interpreted as a time-reversal symmetry of the model. So Livine and Oriti proposed to change the vertex amplitude of the Barrett-Crane model by truncating the sum over ε_f to keep only the term which matches the causal structure of the dual 4-simplicial complex. This defines a causal amplitude with only one term in the asymptotic limit. When Δ consist of many 4-simplices, the same truncation leads to the selection of a single causal structure on Δ .

[1] D. B. Malament, *The class of continuous timelike curves determines the topology of spacetime*, Journal of Mathematical Physics **18**(7), 1399 (1977), doi:[10.1063/1.523436](https://doi.org/10.1063/1.523436).
 [2] C. Rovelli and F. Vidotto, *Covariant Loop Quantum*

Gravity, Cambridge University Press (2014).

[3] A. Ashtekar and E. Bianchi, *A short review of loop quantum gravity*, Rept. Prog. Phys. **84**(4), 042001 (2021), doi:[10.1088/1361-6633/abed91](https://doi.org/10.1088/1361-6633/abed91), arXiv: [2104.04394](https://arxiv.org/abs/2104.04394).

[4] T. Regge, *General Relativity without Coordinates*, Nuovo

- Cim. **19**, 558 (1961), doi:[10.1007/BF02733251](https://doi.org/10.1007/BF02733251).
- [5] J. Engle, E. Livine, R. Pereira and C. Rovelli, *LQG vertex with finite Immirzi parameter*, Nucl. Phys. B **799**, 136 (2008), doi:[10.1016/j.nuclphysb.2008.02.018](https://doi.org/10.1016/j.nuclphysb.2008.02.018), arXiv: [0711.0146](https://arxiv.org/abs/0711.0146).
- [6] E. R. Livine and D. Oriti, *Implementing causality in the spin foam quantum geometry*, Nuclear Physics B **663**(1-2), 231 (2003), doi:[10.1016/S0550-3213\(03\)00378-X](https://doi.org/10.1016/S0550-3213(03)00378-X), arXiv: [gr-qc/0210064](https://arxiv.org/abs/gr-qc/0210064).
- [7] J. Engle, *Proposed proper Engle-Pereira-Rovelli-Livine vertex amplitude*, Phys. Rev. D **87**(8), 084048 (2013), doi:[10.1103/PhysRevD.87.084048](https://doi.org/10.1103/PhysRevD.87.084048), arXiv: [1111.2865](https://arxiv.org/abs/1111.2865).
- [8] J. Engle and A. Zipfel, *The Lorentzian proper vertex amplitude: Classical analysis and quantum derivation*, Phys. Rev. D **94**(6), 064024 (2016), doi:[10.1103/PhysRevD.94.064024](https://doi.org/10.1103/PhysRevD.94.064024), arXiv: [1502.04640](https://arxiv.org/abs/1502.04640).
- [9] S. W. Hawking and G. F. R. Ellis, *The Large Scale Structure of Space-Time*, Cambridge University Press, Cambridge, U.K. (1973).
- [10] P. Dona and S. Speziale, *Asymptotics of lowest unitary $SL(2, C)$ invariants on graphs*, Phys. Rev. D **102**(8), 086016 (2020), doi:[10.1103/PhysRevD.102.086016](https://doi.org/10.1103/PhysRevD.102.086016), arXiv: [2007.09089](https://arxiv.org/abs/2007.09089).
- [11] L. Bombelli, J. Lee, D. Meyer and R. D. Sorkin, *Space-time as a causal set*, Phys. Rev. Lett. **59**(5), 521 (1987), doi:[10.1103/PhysRevLett.59.521](https://doi.org/10.1103/PhysRevLett.59.521).
- [12] S. Surya, *The causal set approach to quantum gravity*, Living Rev. Rel. **22**(1), 5 (2019), doi:[10.1007/s41114-019-0023-1](https://doi.org/10.1007/s41114-019-0023-1), arXiv: [1903.11544](https://arxiv.org/abs/1903.11544).
- [13] M. Cortés and L. Smolin, *Spin foam models as energetic causal sets*, Phys. Rev. D **93**(8), 084039 (2016), doi:[10.1103/PhysRevD.93.084039](https://doi.org/10.1103/PhysRevD.93.084039), arXiv: [1407.0032](https://arxiv.org/abs/1407.0032).
- [14] W. M. Wieland, *A new action for simplicial gravity in four dimensions*, Class. Quantum Grav. **32**(1), 015016 (2015), doi:[10.1088/0264-9381/32/1/015016](https://doi.org/10.1088/0264-9381/32/1/015016), arXiv: [1407.0025](https://arxiv.org/abs/1407.0025).
- [15] W. M. Wieland, *New action for simplicial gravity in four dimensions*, Class. Quantum Grav. **32**(1), 015016 (2015), doi:[10.1088/0264-9381/32/1/015016](https://doi.org/10.1088/0264-9381/32/1/015016), arXiv: [1407.0025](https://arxiv.org/abs/1407.0025).
- [16] G. Immirzi, *Causal spin foams* (2016), arXiv: [1610.04462](https://arxiv.org/abs/1610.04462).
- [17] J. W. Barrett and T. J. Foxon, *Semi-Classical Limits of Simplicial Quantum Gravity*, Class. Quantum Grav. **11**(3), 543 (1993), doi:[10.1088/0264-9381/11/3/009](https://doi.org/10.1088/0264-9381/11/3/009), arXiv: [gr-qc/9310016](https://arxiv.org/abs/gr-qc/9310016).
- [18] J. W. Barrett, *First order Regge calculus*, Class. Quantum Grav. **11**(11), 2723 (1994), doi:[10.1088/0264-9381/11/11/013](https://doi.org/10.1088/0264-9381/11/11/013).
- [19] R. Oeckl, *General boundary quantum field theory: Foundations and probability interpretation*, Adv. Theor. Math. Phys. **12**, 319 (2008), doi:[10.4310/ATMP.2008.v12.n2.a3](https://doi.org/10.4310/ATMP.2008.v12.n2.a3), arXiv: [hep-th/0509122](https://arxiv.org/abs/hep-th/0509122).
- [20] C. Teitelboim, *Quantum mechanics of the gravitational field*, Phys. Rev. D **25**(12), 3159 (1982), doi:[10.1103/PhysRevD.25.3159](https://doi.org/10.1103/PhysRevD.25.3159).
- [21] J. C. Baez, *An Introduction to Spin Foam Models of BF Theory and Quantum Gravity*, In H. Gaussterer, L. Pittner and H. Grosse, eds., *Geometry and Quantum Physics*, Lecture Notes in Physics, pp. 25–93. Springer, Berlin, Heidelberg, ISBN 978-3-540-46552-2, doi:[10.1007/3-540-46552-9_2](https://doi.org/10.1007/3-540-46552-9_2) (2000), arXiv: [gr-qc/9905087](https://arxiv.org/abs/gr-qc/9905087).
- [22] G. Ponzano and T. Regge, *Semiclassical limit of Racah coefficients*, In F. Bloch, ed., *Spectroscopy and Group Theoretical Methods in Physics*. North-Holland, Amsterdam (1968).
- [23] P. Martin-Dussaud, *A primer of group theory for Loop Quantum Gravity and spin-foams*, General Relativity and Gravitation **51**(9) (2019), doi:[10.1007/s10714-019-2583-5](https://doi.org/10.1007/s10714-019-2583-5), arXiv: [1902.08439](https://arxiv.org/abs/1902.08439).
- [24] J. Roberts, *Classical 6j-symbols and the tetrahedron*, Geometry & Topology **3**(1), 21 (1999), doi:[10.2140/gt.1999.3.21](https://doi.org/10.2140/gt.1999.3.21), arXiv: [math-ph/9812013](https://arxiv.org/abs/math-ph/9812013).
- [25] C. Rovelli, *Zakopane lectures on loop gravity*, In *PoS (QGQGS 2011)*, vol. 140, p. 003, doi:[10.22323/1.140.0003](https://doi.org/10.22323/1.140.0003) (2011), arXiv: [1102.3660](https://arxiv.org/abs/1102.3660).
- [26] J. W. Barrett, R. J. Dowdall, W. J. Fairbairn, F. Hellmann and R. Pereira, *Lorentzian spin foam amplitudes: Graphical calculus and asymptotics*, Class. Quantum Grav. **27**, 165009 (2010), doi:[10.1088/0264-9381/27/16/165009](https://doi.org/10.1088/0264-9381/27/16/165009), arXiv: [0907.2440](https://arxiv.org/abs/0907.2440).
- [27] J. W. Barrett and I. Naish-Guzman, *The Ponzano-Regge model*, Class. Quantum Grav. **26**(15), 155014 (2009), doi:[10.1088/0264-9381/26/15/155014](https://doi.org/10.1088/0264-9381/26/15/155014), arXiv: [0803.3319](https://arxiv.org/abs/0803.3319).
- [28] M. Christodoulou, M. Långvik, A. Riello, C. Röken and C. Rovelli, *Divergences and Orientation in Spin-foams*, Class. Quantum Grav. **30**(5), 055009 (2013), doi:[10.1088/0264-9381/30/5/055009](https://doi.org/10.1088/0264-9381/30/5/055009), arXiv: [1207.5156](https://arxiv.org/abs/1207.5156).
- [29] J. W. Barrett and L. Crane, *A Lorentzian Signature Model for Quantum General Relativity*, Class. Quantum Grav. **17**(16), 3101 (2000), doi:[10.1088/0264-9381/17/16/302](https://doi.org/10.1088/0264-9381/17/16/302), arXiv: [gr-qc/9904025](https://arxiv.org/abs/gr-qc/9904025).